ISBN: 978-3-95450-231-8 ISSN: 2673-5490 doi: 10.18429/JACoW-IPAC2023-THPL036

OPTIMIZING THE DISCOVERY OF UNDERLYING NONLINEAR BEAM DYNAMICS AND MOMENT EVOLUTION*

L. A. Pocher†, I. Haber, T. M. Antonsen Jr., P. G. O'Shea
University of Maryland, College Park, MD, USA

Abstract

One of the Grand Challenges in beam physics relates to the use of virtual particle accelerators for beam prediction and optimization. Useful virtual accelerators rely on efficient and effective methodologies grounded in theory, simulation, and experiment. This work extends the application of the Sparse Identification of Nonlinear Dynamical systems (SINDy) algorithm. The SINDy methodology promises to simplify the optimization of accelerator design and commissioning by discovery of underlying dynamics. We extend how SINDy can be used to discover and identify underlying differential systems governing the beam's sigma matrix evolution and corresponding invariants. We compare discovered differential systems to theoretical predictions and numerical results. We then integrate the discovered differential system forward in time to evaluate model fidelity. We analyze the uncovered dynamical system and identify terms that could contribute to the growth(decay) of (un)desired beam parameters. Finally, we propose extending our methodology to the broader community's virtual and real experiments.

INTRODUCTION

Nagaitsev *et al.* [1] have enumerated four Grand Challenges enabling future Department of Energy (DOE) High Energy Physics (HEP) programs. Grand Challenge #4 Beam Prediction poses the question: "How do we develop predictive 'virtual particle accelerators'"? We continue to address an aspect of this Grand Challenge in this paper, continuing our work from NAPAC22 studying prediction of beam dynamics, specifically the beam centroid, in rings [2]. Our *aim* is to speed up commissioning and design studies of accelerators by uncovering underlying physics in virtual and real accelerators. Our *approach* is to apply an existing method from the data-driven, nonlinear dynamics community called *S*parse *I*dentification of *N*onlinear *Dy*namics (SINDy) [3, 4] to uncover physics in problems that can't be solved analytically. Here we apply SINDy to a linear accelerator seeking to capture deviations from equilibrium, where deviations away from the an ideal solution are not captured analytically.

This method is both *Predictive* and *Productive*. The method is predictive in the context of providing an end result model that can be used to predict beam dynamics beyond the training dataset; the method is productive in the context of producing interpretable, physics-based equations predicted upon provided basis functions. In this work be build upon the work of our collaborators at the University of Maryland [5] who use an adjoint technique to optimize the locations and strengths of a flat to round (FTR) to solenoid lattice, Fig. 1, based on an figure of merit. In their work, they assumed an idealized Kapchinsky–Vladimirsky (K-V) distribution and integrated that forward along the lattice solving the moment equations with space charge.

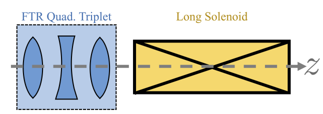

Figure 1: Flat to Round transformation beamline analyzed in Ref. [5]. The four lattice elements consist of the first FTR quadrupole q_0, the second FTR quadrupole q_1, and the third FTR quadrupole q_2, and the long solenoid.

In our work here we use a particle in cell code WARP [6] for a pipe-centered beam at a waist which has the following parameters: 5 keV; 5 mA; $\sqrt{\langle x^2 \rangle} = 2.26$ mm; $\sqrt{\langle y^2 \rangle} = 0.226$ mm; $\varepsilon_x = 64.1$ µm, $\varepsilon_x = .641$ µm. The WARP simulation had the following numerical parameters: pipe radius = 500 mm; grid resolution $N_x = N_y = 2048$; number of particles $N_p = 400$ k; and step size $dz = .1$ mm. The hard-edged lattice parameters are summarized in Table 1.

Table 1: Lattice Parameters for FTR → Solenoid.

Element	Start [mm]	Length [mm]	Strength
Quad 0	4.2	10	-0.2087 T/m
Quad 1	134.6	10	0.2509 T/m
Quad 2	225.2	10	-0.1992 T/m
Solenoid	240.7	200	17 Gs

Two different distributions with the same moments were chosen to highlight how differences between initial distributions affect downstream beam dynamics: the K-V distribution and a rectangular distribution of the following form, when $|x|/\sqrt{\langle x^2 \rangle} < \sqrt{3/2}$ and $|y|/\sqrt{\langle y^2 \rangle} < \sqrt{3/2}$ (forming a rectangle in configuration space),

$$f_{\text{Rect.}}(x, x', y, y') = \frac{1}{8\pi^2 A} \exp\left[-\frac{1}{2}\left(\frac{x'^2}{\langle x'^2 \rangle} + \frac{y'^2}{\langle y'^2 \rangle}\right)\right] \quad (1)$$

where x, x', y, y' denote the usual trace space variables (phase space momentum $p_x \to x'$ via the paraxial approximation), and $A = \sqrt{\langle x^2 \rangle \langle x'^2 \rangle \langle y^2 \rangle \langle y'^2 \rangle}$. These two different distributions are qualitatively compared to each other in Figs. 5(a) and 5(b). It was noted that the moments between the different distributions and those of the moment code

* Work supported by US DOE-HEP grants: DE-SC0010301 and DE-SC0022009.
† lpocher@umd.edu

ISBN: 978-3-95450-231-8 ISSN: 2673-5490 doi: 10.18429/JACoW-IPAC2023-THPL036

matched quite well. However, trace space images produced by the different distribtuions showed significant variations.

SINDy was used to capture the analytic equations governing the difference between the moment code's values for $\langle x^2\rangle(z)$ and $\langle y^2\rangle(z)$ and the WARP K-V result. In this work we explore the results of how this deviation can be back projected onto perturbations to the envelope equation.

APPROACH

Our approach is to prescribe a mathematical model based upon underlying accelerator physics. SINDy works by assuming one can model the evolution of some n-dimensional state vector $\mathbf{x} \in \mathbb{R}^n$ as a system of ordinary differential equations

$$d\mathbf{x}/dt = \mathbf{f}(\mathbf{x}). \tag{2}$$

The variable t is the independent variable, $\mathbf{x}$ is the n-dimensional state vector of observables either from a simulation or experiment, and $\mathbf{f}(\mathbf{x})$ is the n-dimensional function governing the evolution of $\mathbf{x}$.

After one designates the number n of state variables, one can then take measurements of $\mathbf{x}$ at m equidistant times $t_j \in \{t_1, t_2, \ldots, t_m\}$, placing the measurements into a rectanglualr matrix $\mathbf{X}$:

$$\mathbf{X} = \begin{bmatrix} \mathbf{x}^T(t_1) \\ \vdots \\ \mathbf{x}^T(t_m) \end{bmatrix} = \begin{bmatrix} x_1(t_1) & \ldots & x_n(t_1) \\ \vdots & \ddots & \vdots \\ x_1(t_m) & \ldots & x_n(t_m) \end{bmatrix}.$$

One then differentiates the matrix $d\mathbf{X}/dt = \dot{\mathbf{X}}$ which is then used in the discovery stage of SINDy. One proposes a candidate $\Theta(\mathbf{X})$ which consists of a number of intuited/desired basis functions for the underlying dynamics. The matrix $\dot{\mathbf{X}}$ is equated to $\Theta(\mathbf{X})$ times a *sparse* coefficient matrix $\Xi = \left[\xi_0 \; \xi_1 \ldots \xi_{BF}\right]$ which is solved with a given optimization technique

$$\dot{\mathbf{X}} = \begin{bmatrix} \dot{\mathbf{x}}^T(t_1) \\ \vdots \\ \dot{\mathbf{x}}^T(t_m) \end{bmatrix} = \begin{bmatrix} \dot{x}_1(t_1) & \ldots & \dot{x}_n(t_1) \\ \vdots & \ddots & \vdots \\ \dot{x}_1(t_m) & \ldots & \dot{x}_n(t_m) \end{bmatrix} = \Theta(\mathbf{X})\Xi\,.$$

Adapting this framework for beam physics can be done by taking Eq. (2) and transforming the time variable t to the axial location variable z via the paraxial approximation, $t \to z/c\beta_z$. We then assume a number of variables to learn; here we set $n = 3$ for ready visualization. We chose two spatial moments of the sigma matrix $\Sigma_{xx} = \langle x^2\rangle$, $\Sigma_{yy} = \langle y^2\rangle$ and the the independent variable z to ensure the learned differential system is autonomous. Thus, we learn the evolution dynamics for $x = \left[z, \langle x^2\rangle, \langle y^2\rangle\right]^T$. Figure 2 shows a direct comparison for the lattice in Fig. 1 solved in the moment code and WARP.

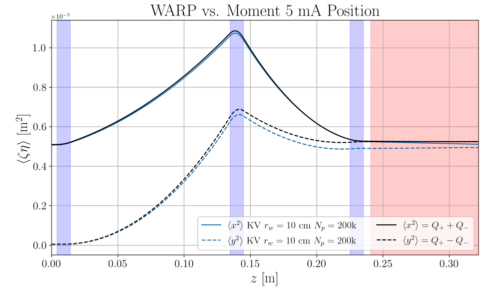

Figure 2: The above plot shows comparisons between WARP and an idealized moment code's results for $\langle x^2\rangle$ and $\langle y^2\rangle$.

THEORY

The envelope evolution equations for an axisymmetric beam may be written as

$$\sigma'' + k_0^2\sigma - \frac{K}{4}\frac{1}{\sigma} - \left(\varepsilon_\sigma^2 + \frac{\langle L\rangle^2}{4p_z^2}\right)\frac{1}{\sigma^3} = 0\,. \tag{3}$$

If one adds a perturbation $\sigma(z) \to \sigma_0 + \delta\sigma(z)$ to Eq. (3) and expands for small $\delta\sigma(z)$ one obtains the following

$$\begin{aligned} &\delta\sigma'' + \delta\sigma f(z;\sigma_0) + \delta\sigma^2 g(z;\sigma_0) \\ &\quad + h(z;\sigma_0) + \mathcal{O}(\delta\sigma^3) = 0\,. \end{aligned} \tag{4}$$

We seek with SINDy to discover the functions $f(z;\sigma_0), g(z;\sigma_0)$, and $h(z;\sigma_0)$. If we select basis functions that correspond to functional forms shown above, we can project how deviations between the idealized moment code result from Dovlatyan *et al.* [5] and WARP occur. These deviations can then be mapped onto an effective moment equation. We note that this heuristic example gives rise to terms that scale with polynomial powers. This result for a perturbation to the idealized moment equation seeds SINDy's $\mathbf{f}(\mathbf{x})$.

First, we nondimensionalize the moment deviations to make the values closer to unity to assist the optimization procedure by not making the entries of the matrix too large

$$\frac{\delta\langle\zeta\eta\rangle}{\langle\zeta\eta\rangle} \equiv \frac{\langle\zeta\eta\rangle_{\text{WARP}} - \langle\zeta\eta\rangle_{\text{mom.}}}{\langle\zeta\eta\rangle_{\text{WARP}}}\,. \tag{5}$$

We assume a profile for FTR quadrupole (de)focusing

$$K_{q_m}(z) = \underbrace{\frac{1}{1 + e^{-\kappa(z - q_{\text{start},m})}}}_{z^- \text{ rise up}} + \underbrace{\frac{1}{1 + e^{\kappa(z - q_{\text{end},m})}}}_{z^+ \text{ fall down}} - 1\,. \tag{6}$$

The nondimensionalization, Eq. (5), and the assumed quadrupole profile, Eq. (6), seed SINDy's $\mathbf{f}(\mathbf{x})$ with polynomial terms going to second order

$$\begin{aligned} f_l(\mathbf{x}) \approx &\underbrace{\sum_{i,j,k=0}^{2}\left[\xi_{\text{poly.}}\, z^i \left(\delta\langle x^2\rangle/\langle x^2\rangle\right)^j \left(\delta\langle y^2\rangle/\langle y^2\rangle\right)^k\right]}_{\text{polynomial}} \\ &+ \underbrace{\sum_{i,j,m=0}^{2}\left[\xi_{\text{quad.}} \left(\delta\langle x^2\rangle/\langle x^2\rangle\right)^i \left(\delta\langle y^2\rangle/\langle y^2\rangle\right)^j K_{q_m}(z)\right]}_{\text{polynomial + quadrupole}}\,. \end{aligned} \tag{7}$$

ISBN: 978-3-95450-231-8 ISSN: 2673-5490 doi: 10.18429/JACoW-IPAC2023-THPL036

RESULTS

Polynomial

Figure 3 shows the result learned SINDy dynamics of the normalized moment difference, Eq. (5), using only the polynomial terms in Eq. (7). Note that even for this limited dataset of only one trajectory in a lattice of 0.3 m how the overall structure of the moment deviations can be captured.

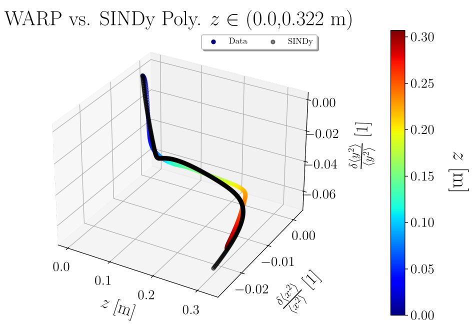

Figure 3: This figure shows the normalized moment difference $\delta\langle\zeta\eta\rangle/\langle\zeta\eta\rangle$ in color and the learned SINDy's learned trajectory in black based on the polynomial basis functions, Eqs. (4) and (7).

Polynomial Plus Quadrupole

Figure 4 shows the result for learned SINDy dynamics of the normalized moment difference, Eq. (5), using only the polynomial terms in Eq. (7). Note how the first twist in the data occuring at 5 mm along the beamline is more accurately captured than in Fig. 3. However, there is a larger deviation from the overall trajectory at the second twist. Larger data sets with more trajectories for the beam will assist in reducing such errors, and is a future research avenue.

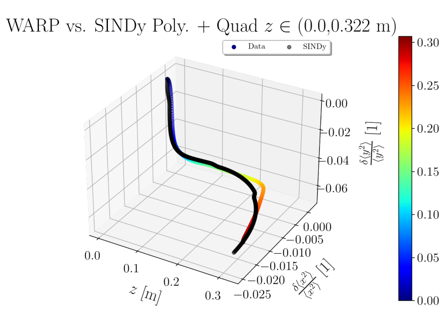

Figure 4: This figure shows the normalized moment difference $\delta\langle\zeta\eta\rangle/\langle\zeta\eta\rangle$ in color and the learned SINDy's learned trajectory in black based on the polynomial and polynomial plus quadrupole basis functions, Eqs. (4) and (7).

Comparison between Distributions

Although the overall moments between various distributions and the idealized moment code are similar, the granular structure of the beam's trace space is heavily dependant on the initial distribution. Figures 5(a) and 5(b) shows a direct comparison between an initially K-V beam and an initially Rectangular beam. Thee differences are not captured in only second order moments.

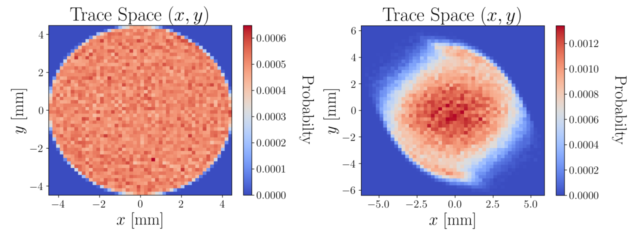

(a) (b)

Figure 5: Configuration space comparison for 5 keV, 5 mA beams. (a) K-V (x, y) projection. (b) Rect. (x, y) projection.

A deeper understanding of the how differences between theory and real distributions is required to control beam dynamics on a finer scale, a scale that will be approached as beams become more intense.

CONCLUSION

We believe SINDy is a promising method that enables the intensification of accelerator commissioning by uncovering underlying beam dynamics. We have shown both recoverable beam dynamics in rings [2] in prior work and also how deviations from idealized solutions can be captured with interpretable, physics-based functions in a limited dataset. With this methodology we aim to develop a *Predictive* and *Productive* framework for beam dynamics with high fidelity. We have yet to explore how differences between more realistic distributions like the rectangular distribution, Eq. (1), and note that more moments of the matrix will be necessary to close the second moment differential system[1]. We seek to uncover how these moments (and perhaps higher order ones) may be used to compose invariants of motion for the beam that are not tractable analytically [7].

ACKNOWLEDGEMENTS

The authors would like to than Daniel P. Lathrop for collaborative discussions and constructive critiques. Work supported by US DOE-HEP grants: DE-SC0010301 and DE-SC0022009.

REFERENCES

[1] S. Nagaitsev *et al.*, "Accelerator and Beam Physics Research Goals and Opportunities," 2021. doi:10.48550/arXiv.2101.04107

[2] L. A. Pocher, T. M. Antonsen, L. Dovlatyan, I. Haber, and P. G. O, "Optimizing the Discovery of Underlying Nonlinear Beam Dynamics," in *Proc. NAPAC'22*, Albuquerque, NM, USA, 2022, pp. 335–338. doi:10.18429/JACoW-NAPAC2022-TUZE3

[1] The terms corresponding to the emittance ε_σ and angular momentum $\langle L \rangle$ in Eq. (3) are composed of second order moments.

ISBN: 978-3-95450-231-8 ISSN: 2673-5490 doi: 10.18429/JACoW-IPAC2023-THPL036

[3] B. M. de Silva, K. Champion, M. Quade, J.-C. Loiseau, J. N. Kutz, and S. L. Brunton, "Pysindy: A Python package for the Sparse Identification of Nonlinear Dynamics from Data," 2020. doi:10.48550/arXiv.2004.08424

[4] A. A. Kaptanoglu *et al.*, "Pysindy: A comprehensive Python package for robust sparse system identification," *Journal of Open Source Software*, vol. 7, p. 3994, 2022. doi:10.21105/joss.03994

[5] L. Dovlatyan, B. Beaudoin, S. Bernal, I. Haber, D. Sutter, and T. Antonsen Jr, "Optimization of flat to round transformers with self-fields using adjoint techniques," *Physical Review Accelerators and Beams*, vol. 25, p. 044 002, 2022. doi:10.1103/PhysRevAccelBeams.25.044002

[6] D. P. Grote, A. Friedman, J.-L. Vay, and I. Haber, "The WARP Code: Modeling High Intensity Ion Beams," in *AIP Conference Proceedings*, American Institute of Physics, vol. 749, 2005, pp. 55–58.

[7] G. Rangarajan, A. Dragt, and F. Neri, "Generalized Emittance Invariants," in *Proc. PAC'89*, Chicago, IL, USA, Mar. 1989, pp. 1280–1283.